Provided for non-commercial research and education use.
Not for reproduction, distribution or commercial use.

(This is a sample cover image for this issue. The actual cover is not yet available at this time.)

This article appeared in a journal published by Elsevier. The attached copy is furnished to the author for internal non-commercial research and education use, including for instruction at the authors institution and sharing with colleagues.

Other uses, including reproduction and distribution, or selling or licensing copies, or posting to personal, institutional or third party websites are prohibited.

In most cases authors are permitted to post their version of the article (e.g. in Word or Tex form) to their personal website or institutional repository. Authors requiring further information regarding Elsevier's archiving and manuscript policies are encouraged to visit:

http://www.elsevier.com/copyright

Author's personal copy

Journal of Theoretical Biology 277 (2011) 27–40

Contents lists available at ScienceDirect

Journal of Theoretical Biology

journal homepage: www.elsevier.com/locate/yjtbi

A mathematical model of combined *bacillus Calmette-Guerin* (BCG) and interleukin (IL)-2 immunotherapy of superficial bladder cancer

Svetlana Bunimovich-Mendrazitsky [a,b,*], Jean Claude Gluckman [c], Joel Chaskalovic [b,d]

[a] *Tel-Aviv University, Israel*
[b] *Ariel University Center, Mathematical Department, Israel*
[c] *INSERM/CNRS/Université Paris Diderot, Institut Universitaire d'Hématologie, U944/UMR7212, Hôpital Saint Louis, 1 avenue Claude Vellefaux 75475 Paris Cedex 10, France*
[d] *Université Pierre et Marie Curie Paris VI, Institut Jean le Rond d'Alembert France*

ARTICLE INFO

Article history:
Received 9 February 2010
Received in revised form
8 February 2011
Accepted 8 February 2011
Available online 18 February 2011

Keywords:
Bladder cancer
BCG immunotherapy
BCG and IL-2 combined therapy
Immune system cells dynamics

ABSTRACT

We report a mathematical model that describes the growth of superficial bladder cancer and the effect thereupon of immunotherapy based on the administration of *Bacillus Calmette-Guerin* (BCG) combined or not with interleukin-2 (IL-2). Intravesical instillations of BCG performed after surgical removal of tumors represents an established treatment with approximately 50% success rate. So far, attempts to improve this efficiency have not led to essential changes. However, convincing clinical results have been reported on the combination of IL-2 to BCG, even though this is still not applied in current practice. The present model provides insights into the dynamical outcomes arising in the bladder from the interactions of immune cells with tumor cells in the course of BCG therapy associated or not with IL-2. Specifically, from the simulations performed using seven ordinary and non-linear differential equations we obtained indications on the conditions that would result in successful bladder cancer treatment. We show that immune cells –effector lymphocytes and antigen-presenting cells–expand and reach a sustainable plateau under BCG treatment, which may account for its beneficial effect, resulting from inflammatory "side-effects" which eliminate residual or eventual newly arising tumor cells, providing thus protection from further cancer development. We find, however, that IL-2 does not actually potentiate the effect of BCG as regards tumor cell eradication. Hence, associating both under the conditions simulated should not result in more efficient treatment of bladder cancer patients.

© 2011 Elsevier Ltd. All rights reserved.

1. Introduction

Immunotherapy of superficial bladder cancer by intravesical instillations of Bacillus Calmette-Guerin (BCG) has been used since 1976 (Morales et al., 1976; Martinez-Pineiro and Muntanola, 1977). It is assumed that BCG locally stimulates the immune response to tumor cells, though its modes of action are not yet fully elucidated (Bevers et al., 2004). This is now a recognized treatment (Chopin and Gattegno, 2002), but a significant proportion of tumors still progress and/or recur despite this therapy. One may thus consider adding another agent to BCG in order to improve its efficacy. In this context, interleukin (IL)-2 is a good candidate, inasmuch as its increased urinary levels in BCG-treated patients appear of predictive value even though this is still controversial (de Boer et al., 1992; Kaempfer et al., 1996; Bohle and Brandau, 2003; Yutkin et al., 2007), and it has already been widely utilized for the therapy of cancer (Rosenberg and Lotze, 1986; Schwartzentruber, 1993; Keilholz et al., 1994; Rosenberg, 2008). IL-2 acts on different immune cells, the most prominent of which are T cells and natural killer (NK) cells (Gaffen and Liu, 2004). Shapiro et al. (2007) treated 19 bladder cancer patients with a combination of BCG and IL-2 and, except for the four who continued to smoke after treatment, there were no recurrences over 10-year follow-up. However, such association is generally not applied.

Dynamic modeling is a powerful tool to integrate empirical data from independent sources, make novel predictions, and foretell gaps in current knowledge. The interactions of the immune system with tumor cells have been studied by numerous authors (Kuznetsov et al., 1994; Nani and Freedman, 2000; Kolev, 2003; Wodarz and Jansen, 2003; Matzavinos et al., 2004; de Pillis et al., 2006; Banerjee, 2008; Isaeva and Osipov, 2009). Several mathematical models have been developed in this respect (Kirschner and Panetta, 1998; Arciero et al., 2004; Cappuccio et al., 2006) not only to understand the specific dynamics of this system but also to optimize therapy (Castiglione and Piccoli, 2006, 2007) and devise new combination therapies (de Pillis et al., 2005).

The first detailed model of the effect of BCG on superficial bladder tumors has been proposed by Bunimovich-Mendrazitsky

* Corresponding author at: Ariel University Center, Mathematical Department, Israel.
E-mail addresses: SvetlanaBu@tauex.tau.ac.il (S. Bunimovich-Mendrazitsky), jean-claude.gluckman@univ-paris-diderot.fr (J. Claude Gluckman), jch@ariel.ac.il (J. Chaskalovic).

0022-5193/$ - see front matter © 2011 Elsevier Ltd. All rights reserved.
doi:10.1016/j.jtbi.2011.02.008

Author's personal copy

et al. (2007). It comprises four ordinary differential equations that characterize the complex biological interactions between BCG, immune cells and tumor cells, which occur then in the bladder. It shows the possibility of obtaining tumor regression without overdriving the immune system, according to the dose of BCG, providing thus the parameters to consider for getting optimal BCG efficiency. Later, Bunimovich-Mendrazitsky et al. (2008) have proposed a simpler model that considers four populations: BCG, effector cells, BCG-infected and uninfected tumor cells. This model allows to study the effects of BCG pulses and to predict conditions for efficient treatment. However, in these models "effector cells" are taken into account only globally without distinguishing the different types of immune cells that are involved in killing tumor cells.

The aims of this paper are twofold: (1) to expand the previous models in order to provide more precise insights into the dynamic processes between different immune cells under the influence of BCG; and (2) to examine *'in silico'* the possible effect of associating IL-2 to BCG in order to determine the conditions under which this could increase the efficacy of BCG treatment.

2. Immunological background

BCG treatment is used after superficial bladder tumors have been surgically removed, at a time when scarce or no tumor cells remain in the urothelium, and only scar fibrosis is found at the location of the removed tumors. The bacteria do not interact with, and thus cannot enter nor infect, normal urothelial cells. Bacteria can contact scar tissue and interact with, and enter into the macrophages, dendritic cells (DCs) –both types being antigen (Ag)-presenting cells (APCs) and polymorphonuclear neutrophil (PMNs) leukocytes that are present there. They can also enter into, and infect the occasional residual cancer cell that remains after surgery, which results in cell death and leads to cell debris and whole or destructed bacteria being captured by local APCs and PMNs via endocytosis or phagocytosis. At any rate, this should have a very weak effect, which would only marginally amplify the immune reactions described below inasmuch as residual cancer cells are scarce at most. However, tumor Ags captured in this manner by APCs may play an important role in initiating the adaptive immune response to tumor cells even if very few events are initially involved since, once initiated, this response corresponds to a quasi-exponential process.

BCG capture by PMNs eventually results in whole bacteria and processed Ags being transferred to DCs (Megiovanni et al., 2006; Morel et al., 2008) and presumably also to macrophages. Through cytokine and chemokine production, these cells cooperate to intensify inflammatory reactions with *ex situ* immune cells, mostly PMNs and macrophages, being recruited *in situ* leading to an innate immune responsiveness "snowball" effect. BCG-activated PMNs can certainly directly kill tumor cells before their own ultimate demise ($\leq$24 hrs), but the other cells involved carry-on for a few days longer.

Macrophages are major targets of mycobacteria (Glickman and Jacobs, 2001). Upon activation by BCG, they produce inflammatory cytokines and chemokines, leading to the recruitment of new PMNs, macrophages and DCs, and increasing the Ag-presenting capacity of the macrophages to T helper (Th) cells in the course of secondary adaptive immune responses, which would occur after the first BCG instillation in patients previously immunized by BCG vaccination or at least after the second instillation. BCG may remain for many days inside macrophages, but this eventually results in lethal bacterial growth and replication, with release of cell debris and whole or destructed bacteria being captured by more macrophages (some bacteria being then destroyed, others being still infectious), PMNs and DCs, which amplifies the reactions. Activated but non-infected neighboring macrophages can directly kill tumor cells.

Although BCG enters into DCs, these are not permissive to mycobacteria growth and replication (Tailleux et al., 2003) and, thus, they are not infected by BCG, properly speaking. BCG in DCs increases the Ag-presenting capacity of the DCs to Th and cytotoxic T lymphocytes (CTLs). It is probable that BCG in DCs would also activate them to produce inflammatory cytokines and chemokines, the consequences of which are reported above.

Even if few, NK cells should play a role in the innate immune response to BCG. Cross-talk between DCs and NK cells reciprocally activates both (Waltzer et al., 2005). Beside their potential killer activity for infected cells, which in the case of BCG should not be of primary importance, NK cells produce, and are activated by interferon (IFN)-γ and IL-2 in particular, which activate Th1 cells and CTLs in the subsequent adaptive immune response. Beside NK cells, NKT cells are special CTLs that recognize glycolipid Ags of the BCG surface. They share properties with 'classical' T cells and with NK cells and are, thus at the crossroad of innate and adaptive immunity. They kill mycobacteria-infected cells without the delay necessary for priming and, when activated, proliferate like T cells, which will subsequently enhance their response (Kronenberg, 2005).

Altogether, the first and possibly major effect of BCG is to activate an innate immune inflammatory reaction with local recruitment of additional immune cells (PMNs, macrophages, DCs, lymphocytes etc …) resulting in positive feedback. This is akin, though much stronger, to the effect of an adjuvant used in a vaccine to trigger the adaptive immune response to Ags. Of note, some inflammatory cytokines can directly stress and kill tumor cells. This effect should continue during implementation of the adaptive immune response and amplify the latter until it tapers.

The adaptive immune response is initiated by APCs that have internalized BCG and/or killed tumor cell debris, processed the corresponding Ags and, getting thus activated, migrated to the draining lymphoid tissues where they present the Ags to CD4+ Th cells via MHC class II molecules or to CD8+ CTLs via MHC class I molecules. BCG glycolipid Ags are also presented to NKT cells via CD1 molecules. Consequently, the activated lymphocytes migrate to the bladder wall. There, a Th1 response develops against BCG-infected and uninfected tumor cells, with production of IFN-γ, IL-2 and TNF-α, cytokines that promote delayed-type hypersensitivity, CTL responses, further macrophage and DC activation and increased inflammation. Depending on bacterial and host components, a Th2 response may occur, with IL-4, IL-6 and IL-10 production, which can balance the Th1 response. The adaptive immune response plays an important role by killing new tumor cells that would eventually arise later. In this context, by initiating a strong inflammatory response BCG should then play the role of a very powerful adjuvant that elicits subsequent strong memory Th and CTL responses against tumor Ags.

Primary adaptive cellular immune responses take two to three days to start being effective (the time for APCs to travel to the draining lymphoid tissue and subsequently for the T cells to arrive at the site of the immune response) with a peak or plateau appearing after one week. Even memory responses take two to three days to be fully effective. Actually, the immune response is finite, and negative feedback mechanisms are activated after five to seven days to taper this response, which, since then, had increased almost exponentially since the responding activated T cells divide and, thus, expand continuously until the process is checked. After a while, if the positive signals are not strong enough, negative signals may take over, leading to tolerance of tumor cells. Therefore, the stimuli provided by immunotherapy have to be well balanced.

Author's personal copy

It may be assumed that adding exogenous IL-2 to BCG will first activate NK cells –and thus augment innate immunity– and thereafter CD4+ and CD8+ T cells, amplifying adaptive responses to BCG as well as to tumor Ags. Of note, IL-2 also activates regulatory T (Tregs) cells (Sakaguchi et al., 2008) the role of which is to dampen Th cell and CTL activity and, thus, reduce the adaptive response. Therefore, in addition to eliciting possible 'toxic' side-effects, the dose of IL-2 used for therapy should take into account this dual effect in order to keep the proper balance between the activities of these T cell types.

3. Materials and Methods

Our mathematical model describes the effects of combining BCG and IL-2 as immunotherapy of bladder cancer with the aim to simulate and, thus, evaluate possible therapeutic scenarios. It is based on current knowledge of the biology of the immune system. However, for the sake of clarity, we did not take into account the distinct interactions between PMNs, macrophages and DCs, but these were taken in as a whole as 'APCs'. For the same reasons, we only considered CTL effector cell activity as the endpoint of the adaptive response and disregarded the help provided by Th cells. Finally, NK cells, NKT cells and Treg cells were not included in the model. Fig. 1 displays the simplified diagram of the immune response used here as deduced from the Immunological Background section there above. Table 1 lists the abbreviations used for the cells and cytokines involved.

The prevailing mathematical models in theoretical immunology involve ordinary differential equations (ODE) to represent reaction kinetics. In general, the equations are used to represent concentrations of molecules or cell populations and the parameters represent kinetic or affinity constants. We considered the tumors to be at early stages or remnants thereof after surgical ablation (superficial bladder cancer), where there are no processes of angiogenesis, invasion and metastasis (which exist at late stages of tumor growth), which would then require a spatial representation of the diffusion of reagents using partial differential equations (PDE). ODEs have been used to model the dynamics of the interactions of immune cells with tumor cells, mainly due to their mathematical simplicity and the long-standing availability of software for solving them.

The model used here consists of seven ordinary differential equations and is extended by taking into account two types of immunotherapy: BCG as an adjuvant therapy and IL-2 as an active therapy. It aims at showing the dynamic processes of different immune cells under the influence of either or both agents and to examine whether IL-2 actually potentiates the effect of BCG. We processed fourth-order Runge–Kutta integration on the differential system to enable numerical simulations. Fourth-order Runge–Kutta integration of the equations was implemented by MATLAB programming, using standard program ODE45 in MATLAB, for a set of initial conditions described in Section 3.1 (after the system (8)). A fractional convergence tolerance of 10^{-5} was applied as the arrest condition of the steepest descent.

3.1. Biological Assumptions and Mathematical Model

The mathematical system we implemented is composed by seven non-linear ODEs to characterize the dynamics of the interactions between the seven different biological components we considered, the local concentrations of which were noted as follows:

- BCG bacteria within the bladder as B,
- APCs (DCs and macrophages) as A,
- activated/matured APC's after BCG internalization and processing as A_1,
- effector T lymphocytes, mostly CTLs that react to BCG and tumor Ags as E,

Table 1
Abbreviations used for the cells and cytokines considered.

Bacillus Calmette-Guerin	BCG
Interleukin -2	IL-2
Antigen (Ag)-presenting cells	APCs
Dendritic cells	DCs
Polymorphonuclear neutrophils	PMNs
Natural killer cells	NK
Cytotoxic T lymphocytes(CD8+ T-cells)	CTLs
Interferon γ	IFN-γ
Lymphoid cells which recognize glycolipid Ags on the BCG surface	NKT

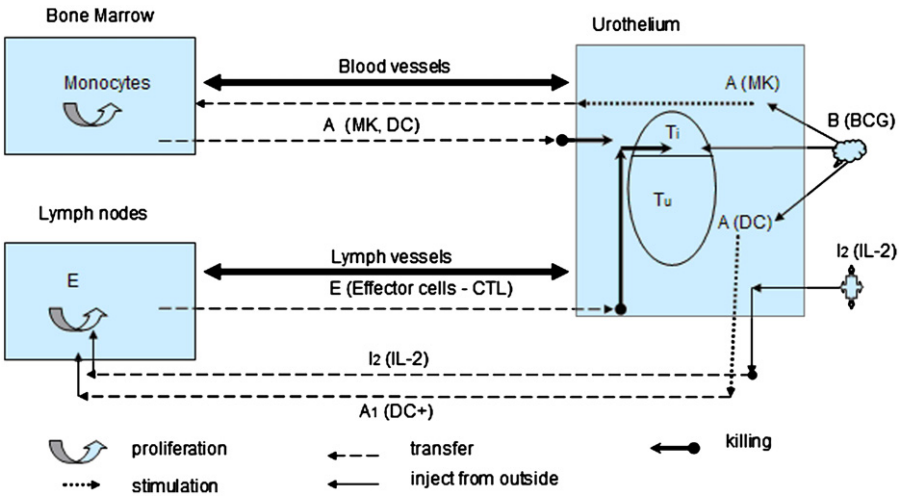

Fig. 1. Summary of the biological assumptions at the basis of the model. BCG is taken up by APC (macrophages (MK) and DC). BCG-activated MK and DCs release cytokines that recruit additional MK and DC from the blood. Activated DCs (DC+) migrate to draining lymph nodes where they present BCG antigens to T cells (indicated here as E (effector CTL cells), which results in their activation and subsequent proliferation. These will then migrate to the site of infection/ inflammation, in the bladder, where the adaptive immune response to tumor cells is to take place. Tumor cells comprise BCG-infected T_i (a minority) and uninfected T_u cells.

Author's personal copy

- IL-2 units injected inside the bladder as I_2,
- tumor cells infected with BCG as T_i,
- tumor cells that are not infected by BCG as T_u.

3.1.1. BCG dynamics

BCG is instilled into the bladder via a catheter inserted through the urethra. In mathematical terms (Schwartz, 1966), discrete time instillation can be represented by Dirac function as input $\delta(t-n\tau)$, where Dirac function equal to 1 to each time $t=n\tau$ and 0 elsewhere. By modeling the instillation as a Dirac function, $(b\delta(t-n\tau))$, we assume that the nth dose, immediately after the given injection, raises $B(t)$ by exactly b units at each specific time $t=n\tau$.

After instillation, BCG accumulates close to the bladder wall. Upon binding to wall cells, BCG is internalized into the bladder and is processed by APCs at rate p_1 (Wigginton and Kirschner, 2001). We also consider that, simultaneously, BCG binds and enters into malignant tumor cells at rate p_2 (de Boer et al., 1992; Durek et al., 1999). BCG concentration decreases as a result of both natural decay and uptake by cells (with half life of μ_B^{-1}).

These mechanisms lead us to write the corresponding mathematical interpretation:

$$\frac{dB}{dt} = \sum_{n=0}^{N-1} b\delta(t-n\tau) - p_1 AB - p_2 BT_u - \mu_B B, \tag{1}$$

where N denotes the number of BCG instillations for a given treatment. In clinical practice N typically varies from 6 to 9 instillations applied every $\tau=7$ days.

3.1.2. Immune response dynamics

3.1.2.1. APC dynamics. APCs are normally present in the bladder and have a natural turnover: a source γ of new cells coming into the site is due to monocyte differentiation and to the natural death (half-life) of cells (at rate μ_A). In the absence of infection, the APC population should remain at equilibrium, $A^*=\gamma/\mu_A$. As a result of infection, APCs undergo two different dynamics: activation/maturation, on the one hand, and enhanced recruitment, on the other hand.

When bacteria are present, additional resting APCs are recruited locally at rate η in response to activated and infected APCs. BCG is readily internalized by both DCs and macrophages at rate p_1.

Based on this phenomenology, one can write the following equation, which drives APCs:

$$\frac{dA}{dt} = \gamma + \eta AB - \mu_A A - p_1 AB. \tag{2}$$

3.1.2.2. Activated APC dynamics. The activation of APCs by BCG (activated APCs$=A_1$) mainly depends on the following mechanisms: first, A_1 production rate $p_1$is assumed to be proportional to the number of APCs, as well as to BCG concentration, and also to migration of the infected and activated APCs to the draining lymphoid tissues (Marino and Kirschner, 2004) where, by the signals they release, they recruit naive Ag-specific T lymphocytes to become activated effector cells.

As a consequence, infected APCs, which do not migrate to lymphoid tissues and continue to phagocytose, are killed by effector cells at rate p_3 (Marino and Kirschner, 2004). Finally, activated APCs that have migrated to lymphoid tissues undergo natural death at rate μ_{A1} after interacting with lymphocytes (apoptosis after maturation).

The resulting equation, which models these mechanisms, is as follows:

$$\frac{dA_1}{dt} = p_1 AB - \beta_1 A_1 - p_3 EA_1 - \mu_{A_1} A_1. \tag{3}$$

3.1.2.3. Effector CTL dynamics. Effector CTLs differentiate from naive T lymphocytes in lymphoid tissues and migrate to infected area in response to signals released by infected and activated APCs A_1. There, they kill BCG-infected and uninfected tumor cells. IL-2, I_2, activates effector CTLs and stimulates their proliferation. Subsequently, we note as β the rate of effector CTL formation described in the quantity $\beta A_1 I_2$. We note that the negative production rate of effector CTLs is related to their inactivation via encounter with T_i, (at rate p_5) and with infected APCs (at rate p_4).

CTLs survive many hits with target cells until they are deactivated and die (Berke, 1994; G. Berke, personal communication; Zagury et al., 1975). We use this fact that one effector cell can kill up to seven infected APCs. Hence, knowing the value of p_3, p_4 was calculated from the above approximations and is shown in Table 2.

Table 2
List of all parameters.

Parameter	Physical Interpretation (units)	Estimated value	Reference
μ_A	APC half life $[days^{-1}]$	0.038	Ludewig et al., 2004
μ_{A1}	Activated APC half life $[days^{-1}]$	0.138	Marino and Kirschner, 2004
μ_E	Effector cells mortality rate $[days^{-1}]$	2.0×10^{-2}	dePillis et al., 2006
μ_B	BCG half life $[days^{-1}]$	0.1	Archuleta et al., 2002
p_1	The rate of BCG binding with APC $[cells^{-1}][days^{-1}]$	1.25×10^{-7}	Wigginton, Kirschner, 2001
p_2	Infection rate of tumor cells by BCG $[cells^{-1}][days^{-1}]$	2.85×10^{-8}	Bunimovich-Mendrazitsky, 2007
p_3	Rate of destruction of infected APC cells by effector cells $[cells^{-1}][days^{-1}]$	0.6×10^{-5}	Ludewig et al., 2004
p_4	Rate of E deactivation after binding with infected APC cells $[cells^{-1}][days^{-1}]$	9×10^{-7}	From model calculations
p_5	Rate of E deactivation after binding with infected tumor cells $[cells^{-1}][days^{-1}]$	1.03×10^{-6}	Kuznetsov et al., 1994
p_6	Rate of destruction of infected tumor cells by effector cells $[cells^{-1}][days^{-1}]$	3×10^{-8}	Kuznetsov et al., 1994
β	Rate of effector cell formation $[cells^{-1}][days^{-1}]$	9.9×10^{-9} 1.12×10^{-8}	Isaeva and Osipov, 2009
γ	Initial APC cells numbers $[cells^{-1}][days^{-1}]$	$4\times10^3-9\times10^3$	Marino, Kirschner, 2004
η	Rate of recruited additional resting APCs $[cells^{-1}][days^{-1}]$	2.8×10^{-6}	Ludewig et al., 2004
r	Tumor growth rate $[days^{-1}]$	0.0033 0.012 0.0078	Shochat et al., 1999; Swanson et al., 2003; In all simulations
B	Bio-effective concentration of BCG [c.f.u./day]	10^5-10^7	Bunimovich-Mendrazitsky, 2007
β_1	Rate of recruitment of effector cells in response to signals released by infected and activated APC$[cells^{-1}][days^{-1}]$	0.0341	Ludewig et al., 2004

Author's personal copy

We assume μ_E as the constant natural death rate. Then, one can model the dynamics of effector cells as follows:

$$\frac{dE}{dt} = \beta A_1 I_2 - p_5 T_i E - p_4 E A_1 - \mu_E E. \quad (4)$$

3.1.2.4. IL-2 dynamics. IL-2 is mainly produced by activated T lymphocytes. Its half-life when administered intravenously is of only about 10 minutes due to its rapid distribution into the organism total extracellular space. During the process, when APCs present BCG antigens to Th cells, IL-2 is produced at rate q_1. In lymphoid tissues, IL-2 promotes differentiation into effector CTLs at rate q_2 after APCs have activated T lymphocytes. However, rate β in (4) is not equal to rate q_2, because IL-2 is used for activating other cells too (Malek and Bayer, 2004) such, for example, as NK cells.

We also introduce μ_{I2} as IL-2 loss/degradation rate.

Last, we note as i_2 IL-2 external source, which is injected into the bladder every τ time units and which is assumed to degrade rapidly without the possibility to having systemic effects. Injections are modeled in the same manner as for BCG by using the Dirac function $i_2\delta(t-n\tau)$. For the time $t=n\tau$ Dirac function equal to 1 and IL-2 is injected, otherwise Dirac function equal to 0 and no treatment pulse.

So, evolution of IL-2 concentration in the bladder is given by:

$$\frac{dI_2}{dt} = q_1 A_1 - q_2 I_2 - \mu_{I_2} I_2 + \sum_{n=0}^{N-1} i_2 \delta(t-n\tau), \quad (5)$$

where N denotes the number of IL-2 instillations we consider for a given treatment.

3.1.3. Tumor cell dynamics

Our model considers two subpopulations: BCG-infected (T_i) and uninfected (T_u) tumor cells.

3.1.3.1. Infected tumor cells. The dynamics of infected tumor cells depends on two mechanisms. The first corresponds to infection of uninfected tumor cells T_u by the bacteria at rate p_2; the second is due to the interaction with CTL effectors E, which destroy infected tumor cells T_i at rate p_6 because T_i cells express BCG Ags. Of note, BCG has an anti-proliferative effect on human urothelial carcinoma cell lines; therefore infected tumor cells should not increase in number (Bevers et al., 2004; Bevers personal communication; Chen et al., 2005).

Therefore, one can model the dynamics of infected tumor cells as follow:

$$\frac{dT_i}{dt} = p_2 B T_u - p_6 E T_i. \quad (6)$$

Table 3
List of parameters for IL-2.

Parameter	Physical Interpretation(units)	Estimated value	Reference
q_1	Rate of IL-2 production $[cells^{-1}][days^{-1}]$	$.45\times10^{-3}$ 5×10^{-3}	Castiglione and Piccoli, 2006; Banerjee, 2008
q_2	Rate of CTL differentiation $[cells^{-1}][days^{-1}]$	5×10^{-8} 6.6×10^{-8}	Castiglione and Piccoli, 2007; Isaeva and Osipov, 2009
μ_{I_2}	Degradation rate $[days^{-1}]$	0.1	Castiglione and Piccoli, 2007
i_2	Rate of external source [units per treatment]	8×10^5–7.7×10^6	Shapiro et al., 2007

3.1.3.2. Uninfected tumor cells. The number of T_u cells increases due to the balance between their natural exponential growth rate, noted r, and their infection by BCG at rate p_2 during BCG therapy. The tumor cells become infected with BCG at rate p_2BT_u where p_2 is a rate coefficient.

We assume that, in the absence of BCG, uninfected tumor cells T_u undergo exponential growth, with growth rate r.

As a consequence, the dynamics of uninfected tumor cells is as follows:

$$\frac{dT_u}{dt} = rT_u - p_2 B T_u. \quad (7)$$

Thus, the interactions of BCG and IL-2 with the immune cells are modeled by the following system composed of seven ordinary nonlinear differential equations:

$$\begin{cases} \frac{dB}{dt} = \sum_{n=0}^{N-1} b\delta(t-n\tau) - p_1 AB - p_2 B T_u - \mu_B B, & (1)\\ \frac{dA}{dt} = \gamma + \eta AB - \mu_A A - p_1 AB, & (2)\\ \frac{dA_1}{dt} = p_1 AB - \beta_1 A_1 - p_3 E A_1 - \mu_{A_1} A_1, & (3)\\ \frac{dE}{dt} = -\mu_E E + \beta A_1 I_2 - p_5 T_i E - p_4 E A_1, & (4)\\ \frac{dI_2}{dt} = q_1 A_1 - q_2 I_2 - \mu_{I_2} I_2 + \sum_{n=0}^{N-1} i_2 \delta(t-n\tau), & (5)\\ \frac{dT_i}{dt} = p_2 B T_u - p_6 E T_i, & (6)\\ \frac{dT_u}{dt} = rT_u - p_2 B T_u. & (7) \end{cases} \quad (8)$$

As for every dynamic system, we specify the initial conditions at the beginning of the process when t=0:

- $B(0)=0$, (BCG is not present at the beginning of the treatment),
- $A(0)=A_0>0$, (A_0 describes the number of APCs that are present before therapy),
- $A_1(0)=E(0)=I_2(0)=T_i(0)=0$, (The immune components and infected tumor cells are zero at the beginning of the process),
- $T_u(0)=T_{u0}(0)>0$, (T_{u0} denotes the uninfected tumor cells in the urothelium).

Remark. Existence, uniqueness and positivity of problem (8) solutions are presented at the end of the paper as a particular case of three general theorems we detailed in the Appendix.

3.2. Estimation of parameters

To complete the mathematical model it is useful to estimate parameter ranges that are realistic and agree with values from the literature. Although this plays some role in the following analysis, we emphasize that our goal is not to derive a predictive simulation model using exact rate parameters. Instead, we aim at finding generic qualitative results that are intrinsic to the model's structure. As our analytical results are not tied to any specific growth rate we do not require precise rate values. This notwithstanding, parameter values are compiled from published experimental data, with weight given to results obtained from humans or human cells and specific data over results based on other species.

Once mathematical expressions were developed representing the interactions between the seven cell populations and IL-2, it was necessary to determine the values of the rate constants governing each interaction. Estimates obtained from multiple studies are represented as value ranges. For parameters with a range and for those without available experimental data, we

Author's personal copy

performed uncertainty and sensitivity analyses to obtain order-of-magnitude estimates as described below.

A summary of the parameter values used here is given in Tables 2 and 3. In this section we discuss the acquisition of the parameters of the unscaled model (Eq. (2)) i.e., before nondimensionalisation.

The data of Aranha et al. (2000) (Fig. 2) are compatible with in vitro bladder cancer cell growth rates of $r \sim 0.37–0.5\ \text{day}^{-1}$ with 1.5–2 days doubling time. However, such large growth rates may be biased as they represent *in vitro* cell growth in favorable medium without the constraints that normally occur *in vivo*. On the other hand, *in vivo* studies report $r = 0.001–0.03\ days^{-1}$ growth rates for breast cancer cells (Spratt et al., 1993; Shochat et al., 1999). Here, we assume that *in vivo* bladder cancer growth rates are smaller than *in vitro*, and the r values we consider for the simulations vary from 0.001 days^{-1} to 0.045 days^{-1}.

Typical values for BCG instillation b were obtained from Cheng et al. (2004) whose patients received weekly doses of $2.2 \times 10^8 - 6.4 \times 10^8$cfu (colony-forming units i.e., number of viable bacteria). Most of these leave the bladder within the first two hours. Brandau (personal communication) estimates that 99% of BCG is lost in this way. A reasonable weekly rate for b is thus in the range of $0.01 \times (2.2 \times 10^8 - 6.4 \times 10^8) = 1 \times 10^6 - 10 \times 10^6$ cfu/week.

Parameter p_2 was estimated by imposing reasonable time scales to the tumor-eradication process (several weeks) as in our previous reports (Bunimovich-Mendrazitsky et al., 2007, 2008).

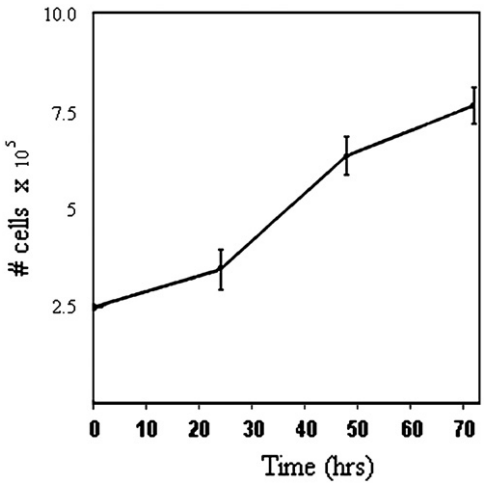

Fig. 2. Tumor cell growth of HTB9 cells in *vitro* (TCC human line, grade II), taken from Aranha et al. (2000). The number of living cells is plotted against incubation time.

According to Lämmle et al. (2002), the maximal radius of bladder tumors, as determined by MRI, ranges from 4 to 64 mm. From this, we calculated the maximal tumor surface area by assuming its shape as circular. It was also assumed that the tumor had a three-cell depth allowing us to evaluate its volume based on the size of a cell being approximately 10 μm. Given that $1\ \text{mm}^3 \sim 10^6$ cells (Spratt et al., 1993), the approximate number of cells per maximal tumor is:

$$T_{uMAX} = \pi r^2 h \times 10^6 \approx \pi \times 64^2 \times 3 \times 10^{-2} \times 10^6 = 3 \times 10^9 \text{ cells.}$$

Here, we assumed initial tumor size before treatment as $T_u = 2 \times 10^6$ cells.

Regarding IL-2, we considered the data of Shapiro et al. (2007) using increasing doses of IL-2 from $6 \times 10^6 - 54 \times 10^6$ units per weekly treatment.

To determine the parameters of IL-2 dynamics and the dynamics of effector cells affected by IL-2, we used studies of Castiglione and Piccoli, (2006, 2007), Banerjee, (2008) and Isaeva and Osipov (2009), which evaluated the dynamics of IL-2 as a result of immunotherapy.

As regards the initial conditions for APCs in our model, we used the figures of Marino & Kirschner (2004) in the lung in particular; i.e. $4.0 \times 10^5 - 5 \times 10^5$ macrophages and $5.0 \times 10^4 - 10.0 \times 10^4$ DCs.

3.3. Sensitivity analysis of parameters

There are differences in the parameter values taken from different sources due to their wide variability. Therefore, a sensitivity analysis was conducted to test which parameters, in the ranges noted in Tables 2 and 3, impacted the most tumor cell numbers in agreement with the model predictions.

We first examined how the initial number of APCs in the bladder (parameter γ) could affect evolution of tumor cells (Fig. 3A). We found that BCG-infected tumor cell numbers decreased as the initial number of APCs was increased from 4×10^3 to 9×10^3, as intended in the model, whereas under the same condition uninfected tumor cell numbers decreased, as if BCG uptake by APCs reduced the amount of free BCG available to infect tumor cells. As expected, the numbers of activated APCs and effector cells varied according to the initial APC numbers, which thus influence the strength of the immune response (Fig. 3B).

We next assessed the effects of different rates of formation of effector cells (parameter β) (Fig. 4). The evolution of effecter cell numbers with time was, as expected, related to their formation rates. Also, BCG-infected tumor cell numbers moved down as β increased, but for the lowest β value tested under which condition these numbers increased.

To evaluate the impact of IL-2 production on the dynamics of effector cells, and *vice-versa*, on the evolution of BCG-infected

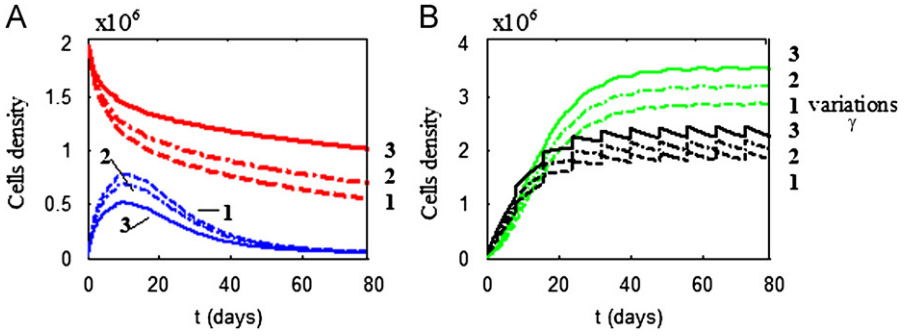

Fig. 3. (A) Evolution with time of uninfected (red lines) and BCG-infected (blue lines) tumor cell numbers in relationship with the initial numbers of APCs (parameter γ) in the bladder over a specified range $[4 \times 10^3 - 9 \times 10^3]$. (B) Evolution with time of activated APCs (black lines) and effector cells (green lines) in relationship with the same parameter. Three values are considered: **1.** $\gamma = 4 \times 10^3$, dashed lines; 2. $\gamma = 6 \times 10^3$, dash-dotted lines; 3. $\gamma = 9 \times 10^3$, solid lines. (For interpretation of the references to color in this figure legend, the reader is referred to the web version of this article.)

Author's personal copy

tumor cell numbers, we varied parameters q_1 and q_2. Increasing parameter q_1 resulted in increased effector cell numbers and lowering of BCG-infected tumor cell numbers with only modest effects on activated APCs (Fig. 5). Surprisingly, effector cell numbers and IL-2 production levels displayed inverse relationships with parameter q_2, which affected only marginally BCG-infected tumor cell numbers (Fig. 6).

3.4. Existence of tumor free equilibrium with side effect

Our interest in this section is to find out equilibrium of ODEs system (8) which corresponds to tumor free state where $T_i^* = T_u^* = 0$, (* denotes the steady state for any considered unknown).

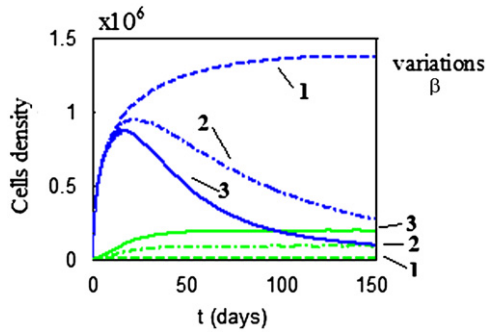

Fig. 4. Evolution with time of BCG-infected tumor cells (blue lines) in relationship with the rate of formation of effector cells (green lines) (parameter β) in the bladder over a specified range $[9.9\times10^{-9}-1.12\times10^{-8}]$. Three values are considered: **1.** $\beta=0.9\times10^{-8}$, dashed lines; 2. $\beta=0.98\times10^{-8}$, dash-dotted lines; 3. $\beta=1.2\times10^{-8}$, solid lines. (For interpretation of the references to color in this figure legend, the reader is referred to the web version of this article.)

To this end, we considered the case where the general pulsing immunotherapy of BCG and IL-2 are changed as constant therapy rates b and i_2. Then, system (8) becomes as follows:

$$\begin{cases} \frac{dB}{dt} = b - p_1AB - p_2BT_u - \mu_B B, \\ \frac{dA}{dt} = \gamma + \eta AB - \mu_A A - p_1AB, \\ \frac{dA_1}{dt} = p_1AB - \beta_1A_1 - p_3EA_1 - \mu_{A_1}A_1, \\ \frac{dE}{dt} = -\mu_E E + \beta A_1I_2 - p_5T_iE - p_4EA_1, \\ \frac{dI_2}{dt} = q_1A_1 - q_2I_2 - \mu_{I_2}I_2 + i_2, \\ \frac{dT_i}{dt} = p_2BT_u - p_6ET_i, \\ \frac{dT_u}{dt} = rT_u - p_2BT_u. \end{cases} \tag{9}$$

We define $X=(B,A,A_1,E,I_2,T_i,T_u)$. Using the parameter values described in the previous section, it is straightforward to show that only one steady states of the system (9) is:

$$X^* = \{B^* = 4.04*10^6; A^* = 5.64*10^8; A_1^* = 11.528*10^6; E^* = 5.7*10^6,$$

$$I_2^* = 9.93*10^6; T_i^* = T_u{}^* = 0\}.$$

Because $E^* \neq 0$, this equilibrium state is characteristic of a residual side effect developed by the immune system.

On the other hand, other numerical solutions we found are not biologically realistic.

Now, to analyze the stability of the equilibrium X^*, we introduce the vector $\Xi=(\xi_1,\xi_2,\xi_3,\xi_4,\xi_5,\xi_6,\xi_7)$as follows:

$$\Xi = X - X^*. \tag{10}$$

By linearizing about the steady state X^*, we obtain the following linear system:

$$\frac{d\Xi}{dt} = J\Xi, \tag{11}$$

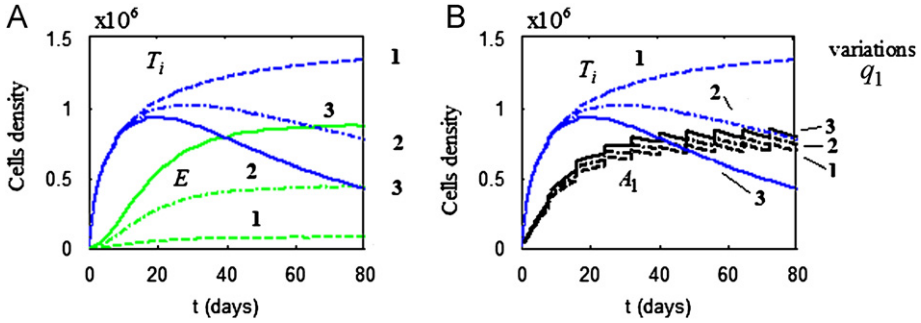

Fig. 5. (A) Evolution with time of effector cells (green lines) and BCG-infected tumor cells (blue lines) in relationship with the level of IL-2 production (parameter q_1) over a specified range $[.45\times10^{-3}-5\times10^{-3}]$. (B) Evolution with time of activated APCs (black lines) and BCG-infected tumor cells (blue lines) in relationship with the same parameter. Three values are considered: **1.** $q_1=0.45\times10^{-3}$, dashed lines; 2. $q_1=2.5\times10^{-3}$, dash-dotted lines; 3. $q_1=5\times10^{-3}$solid lines. (For interpretation of the references to color in this figure legend, the reader is referred to the web version of this article.)

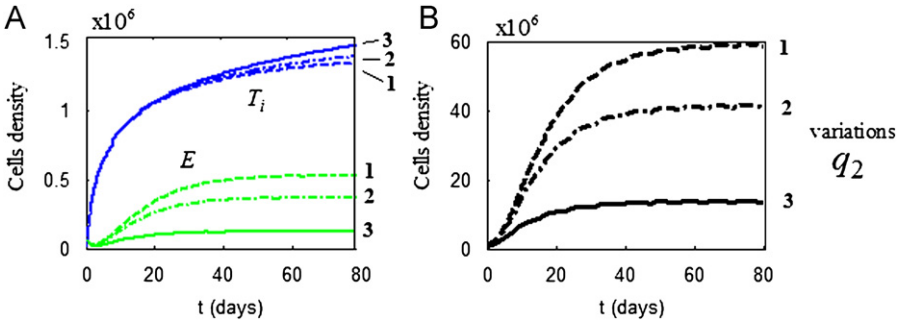

Fig. 6. (A) Evolution with time of effector cells (green lines) and BCG-infected tumor cells (blue lines) in relationship with the rate of CTL differentiation (parameter q_2) over a specified range $[5\times10^{-8}-6.6\times10^{-8}]$. (B) Evolution with time of IL-2 (yellow lines) in relationship with the same parameter. Three values are considered: **1.** $q_2=5\times10^{-8}$, dashed line; 2. $q_2=5.7\times10^{-8}$, dash-dotted lines; 3. $q_2=6.6\times10^{-8}$, solid lines. (For interpretation of the references to color in this figure legend, the reader is referred to the web version of this article.)

Author's personal copy

where J is the Jacobian matrix evaluated at the corresponding steady state X^*. It is straightforward to show that for X^* all eigenvalues of J is negative. Hence, equilibrium X^*, which represents the side-effect tumor free steady state is stable for these specific parameters. As a consequence, in our model, the tumor-free equilibrium without side effects does not exist. Indeed, bladder cancer is rarely cured without side effects resulting from BCG therapy, and progression-free survival has been shown to be significantly higher in patients with major side effects than in those with minor ones (Lamm, 1992; Morales, 1984; Suzuki et al., 2002).

4. Computer simulation and results

4.1. Simulation of the progression of untreated bladder cancer

We first simulated the progression of untreated bladder cancer, for which we set the two parameters b and i_2 to zero values. We also used an exponential tumor growth rate, as for high-grade urothelium carcinoma, with $r=0.0078\ days^{-1}$ (Fig. 7) as explained above.

The initial number of T_u cells was set at 2×10^6, because tumors can grow to a nutrient-limited size of approximately 1–2 mm in diameter (and contain $O(10^6)$ cells) without the need to initiate angiogenesis (Arciero et al., 2004).

The resulting simulation of T_u cell growth given by Eq. (7) is plotted in Fig. 7. The limit value for the number of cells we obtained is around 3×10^9 after about 2 years of free growth (see estimation of parameters). This is in line with data of Kim and Steinberg (2001), Iori et al. (2002) and Knowles (2006), who have estimated that high-grade tumors require 3–5 years to progress from their size at diagnosis (which is in the range we considered) to maximal size at death.

Of note, in this simulation, the number of effector lymphocytes remains close to zero, which directly results from the assumption in the model that their activation would only result from the treatment, *a priori* discounting the evolution of the number of CTLs in response solely to cancer cell antigens.

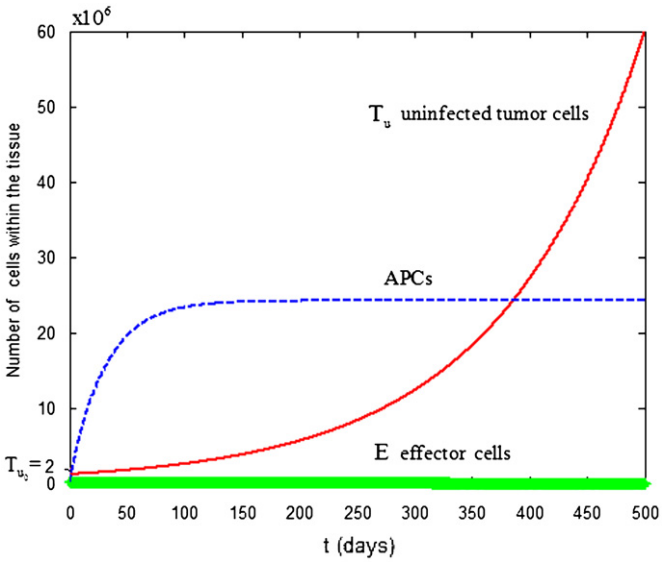

Fig. 7. Simulation of bladder cancer progression in the absence of BCG and IL-2 treatment. Eq. (8) was used, setting $b=0$ and $i_2=0$. The graph shows the evolution with time of T_u (uninfected tumor cells, solid thick line), E (effector cells, solid heavy line), APCs/100 (dashed line). We used an initial tumor population size $T_{u_0}=2\times10^6$ cells. Parameters are from Table 2; tumor growth rate: $r=0.0078$ days^{-1}.

4.2. Influence of BCG on bladder cancer

We next assessed the influence of BCG, without IL-2, on tumor growth. Therefore, we set BCG influx rate as $b=1.6\times10^5$ cfu/day and $i_2=0$ (Fig. 8).

The model shows that a minority of tumor cells will get initially infected by BCG, the number of infected cells T_i initially increasing in a few days after the first instillation and rapidly diminishing, decreasing by about 10-fold before day 20 after initiation of therapy. As to the number of uninfected tumor cell T_u, it progressively decreases and abates to almost zero in about 1 year.

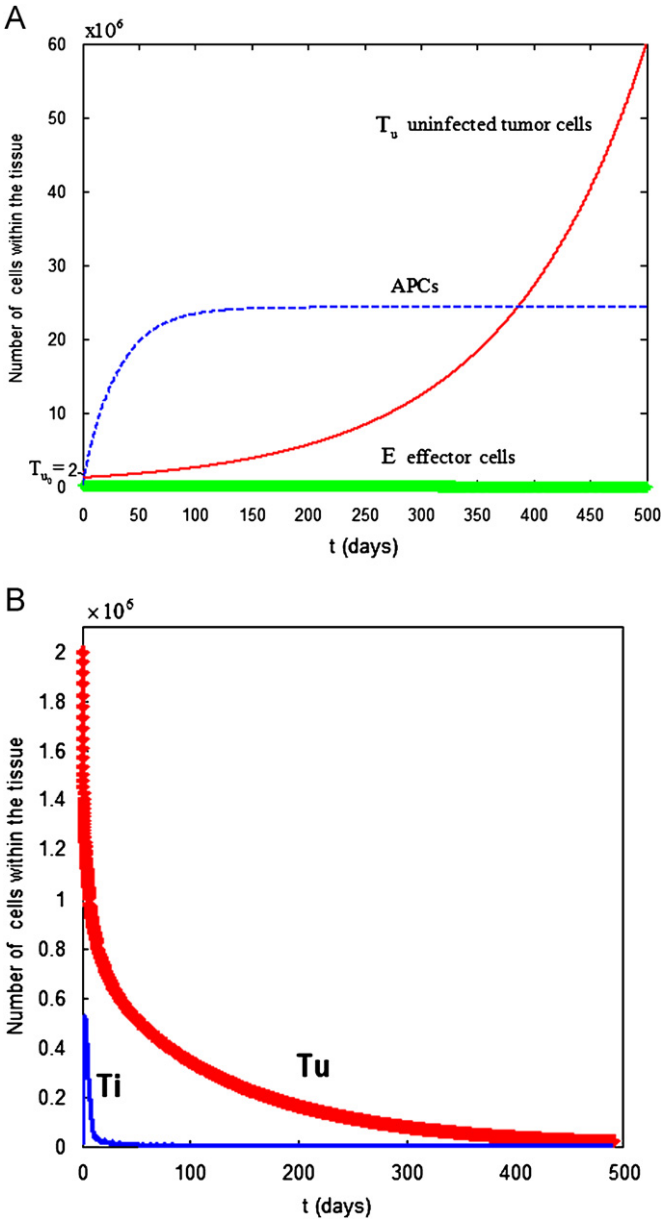

Fig. 8. Simulation of the effects of a treatment regimen with nine BCG instillations ($b=1.6\times10^6$ cfu/day, $i_2=0$) administered every $\tau=7$ days. Evolution with time of the numbers of uninfected tumor cells (T_u: red solid heavy line), BCG-infected tumor cells (T_i: blue solid line), BCG bacteria (black slashed line), effector cells (green dash-dotted line), and activated APCs (yellow dashed line). Evolution for (A) the first 56 days during therapy, and (B) up to 500 days during and after therapy. Parameters are from Table 2; $r=0.007$ days-1. (For interpretation of the references to color in this figure legend, the reader is referred to the web version of this article.)

Author's personal copy

Meanwhile, effector lymphocyte numbers expand and reach a plateau ($E=0.6\times10^6$cells) after treatment day 10. The evolution of activated APCs globally parallels that of effector lymphocytes, which together should account for the noted evolution of tumor cell numbers.

4.3. *Influence of IL-2, administered solely or with BCG, on bladder cancer*

Before examining whether IL-2 could enhance the efficiency of BCG, we assessed how it could affect bladder cancer by itself.

4.3.1. *Effect of IL-2 treatment only without BCG*

It was found that administering only IL-2 did not result in the elimination of tumor cells (Fig. 9A), which continue to progressively grow and proliferate exponentially, at least up to 500 days (Fig. 9B), in the same manner as in the absence of any treatment (see Fig. 7). Meanwhile, APC levels increase during the first three weeks and remain stable thereafter, while effector lymphocyte numbers taper off.

4.3.2. *Effect of combining IL-2 treatment with BCG*

Next, we modelised the effects of a treatment combining BCG and IL-2. The results shown in Fig. 10 are based on use of two doses of IL-2, in the range which is customary in clinical practice, administered in association with the same amount of BCG: $b=1.6\times10^6$ cfu/day. This shows that the result of such combination would not be different from that of treating with BCG only, uninfected tumor cell decreasing then at comparable rates whether IL-2 is added or not (see also Fig. 8). Only when looking at BCG-infected tumor cells does it appear that different decrease kinetics may be noted when IL-2 is increased from 1.1×10^6 (Fig. 10A) to 11×10^6 units (Fig. 10B), the cells being eradicated more rapidly with the higher than with the lower dose (and <20 days without IL-2).

This indicates that, under the conditions assumed, IL-2 does not actually potentiate the effect of BCG as regards overall tumor cell eradication.

4.4. *Asymptotic stable equilibrium of immune cells according to the amounts of BCG or IL-2 administered*

We finally examined the respective dynamics of immune cells in relation with the amounts of BCG and IL-2 injected. To this end, we determined whether a particular and final state of the given cell population, called asymptotic stable equilibrium of the system (marked "*" when referring to the equilibrium value), could be reached under each condition. This state corresponds to the particular value of each variable of the model provided the time period is sufficiently long and the values persist in a sustainable state.

Thus, the effect of varying BCG doses b on effector lymphocyte E^* and activated APC A_1^* equilibrium levels was investigated (Fig. 11A). This reveals that E^* is almost independent of the BCG dose used, which nonetheless appears to directly influence A_1^* which increases linearly. The explanation for this observation should be that BCG directly interacts with APCs but not with effector T cells.

The same was performed regarding IL-2 doses i_2 (Fig. 11B). Here, effector lymphocyte E^* equilibrium levels increases with increasing IL-2 doses whereas APCs A^* and activated APCs A_1^* remain level. This observation should be accounted for by the fact that IL-2 directly activates the effector lymphocytes via their specific receptors but does not directly interact with APCs.

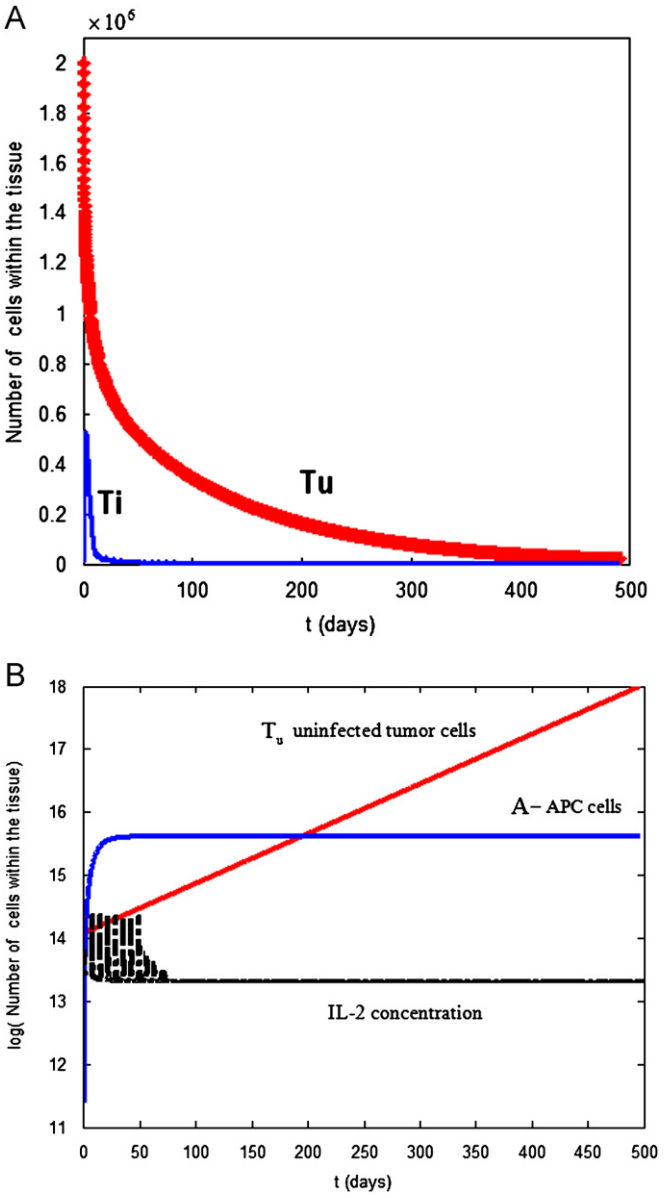

Fig. 9. Simulation of the effects of a treatment regimen with eight IL-2 instillations: ($i_2=10^7$ units per dose) administered every $\tau=7$ days. Evolution with time of the numbers of tumor cells (T_u: red solid heavy line), IL-2 concentration (black slashed-dotted line), effector lymphocytes (green dash-dotted line), and activated APCs (blue solid line). Evolution for (A) the first 50 days during IL-2 therapy, (B) up to 500 days during and after therapy (the y axis is presented in log scale). (For interpretation of the references to color in this figure legend, the reader is referred to the web version of this article.)

5. Discussion

Intravesical BCG instillations remain the best therapy for superficial bladder cancer. However, many high-grade tumors recur and progress despite BCG therapy. Therefore, it is important to continue studying the mechanisms of the immune response to BCG and its effects on urothelial tumor cells. Here, we hypothesized that cytotoxic effector cells play an essential role in the eradication of tumor cells (Bevers et al., 2004). Hence, our model examined the interactions of CTLs with APCs, which affect their function, and with their putative targets (infected or non-infected tumor cells). To investigate the possible additional effect of IL-2, we introduced additional variables in order to analyze the possible effect of this combined immunotherapy and provide a more detailed description of the

Author's personal copy

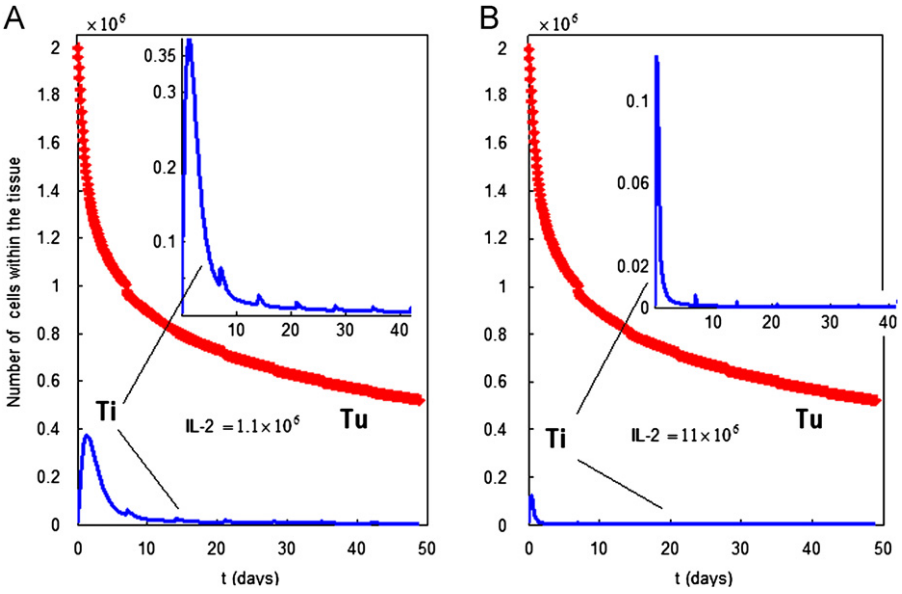

Fig. 10. Simulation of the effects of treatment associating BCG and IL-2. Differential system (8) was used to simulate two treatment regimens, each involving five instillations. Evolution with time of uninfected (T_u: solid line) and BCG-infected tumor cells (T_i: dashed line). (A) Instillations associate doses of IL-2: $i_2=1.1\times10^6$and BCG: $b=2.2\times10^6$. (B) Instillations associate doses of IL-2: $i_2=11\times10^6$ and BCG $b=2.2\times10^6$. Parameters are from Tables 2 and 3, with initial tumor size before treatment $T_u=2\times10^6$.

biology of the system. The results obtained indicate that, under the modeled conditions, IL-2 does not potentiate the effect of BCG as regards overall tumor cell eradication. this conclusion may be based on too limited mimicked conditions but, using different sets of APC, activated APC, CTL and Il-2 parameters, did not change the results. Thus, it is possible that we have next to examine other cell types to more closely mimic the immune response in this setting. For example, IL-2 activates first NK cells (Bohle and Brandau, 2003; Yutkin et al., 2007), which should start then to eradicate tumor-uninfected cells, before acting on T cells. Also, later on NK cell activity depends on Th1 cytokines IFN-γ and IL-12 (Suttmann et al., 2004). This supports a possible critical role for NK cells in mediating the response to BCG. Therefore, we consider introducing NK cells in future models.

The model implemented here is obviously a simplification of a complex biological reality. It does not take into account many immune cell types, saturation effects and the spatial heterogeneity of tumor growth. Also, for our simulations, we used representative values of the kinetic parameters taken from broad ranges reported in the literature. Nevertheless, this model mimics more closely than our previous ones (Bunimovich-Mendrazitsky et al., 2007, 2008) the immune reactions that occur upon treatment of superficial bladder cancer with BCG. There, the interactions of tumor, immune cells and BCG were examined by a four-dimensional system. Here, we have considered additional parameters in order to improve the model and, therefore, the comprehension of the interactions occurring between the bacteria administered, immune cells and tumor cells during such treatment. Hence, we added additional variables, such as APCs and effector lymphocytes, to the model in order to provide a more detailed description of the immune response elicited by, and the effects of the treatment. Second, we modeled another potential immunotherapy regimen in which the effect of the cytokine IL-2, used alone or in association with BCG, was examined.

The present results globally confirm those of the previous reports (Bunimovich-Mendrazitsky et al., 2007, 2008) as regards the outcome of BCG therapy on bladder cancer cells, by showing that, indeed, under the effect of the treatment, the number of tumor cells progressively dwindles to ultimately get eradicated approximately one year after the series of instillations.

In addition, they provide new insight as to the role played by immune cells in the effectiveness of this therapy. Indeed, BCG appears to rapidly infect up to 25% of tumor cells, which are then eliminated in less than three weeks. This process apparently leads to the priming of the immune response to tumor cells that had not been infected by BCG. Thus, both activated APCs and effector lymphocytes persist in the urothelium for a prolonged period, and this should result in the progressive elimination of residual tumor cells and in blocking any potential later cancer development by initiating secondary recall immune responses. Altogether, this local persistence of immune cells accounts fairly well for the clinical effectiveness of BCG treatment.

In contrast, modeling the use of IL-2, solely, shows that the cytokine by itself does not result in clearing tumor cells, which continue to grow exponentially even though APC and effector lymphocyte numbers display approximately similar patterns during the six weeks of treatment in both instances. Of note, and in contrast to that which is noted in the present model, IL-2 therapy is known for its efficacy in other cancers (Kirschner and Panetta, 1998; de Boer et al., 2006).

Simulation of a therapy associating IL-2 to BCG shows no potentiation of the effect of BCG, since overall tumor cell numbers decrease with a similar kinetics whether IL-2 is added or not to BCG. Therefore, associating IL-2 to BCG should not result in more efficient treatment of superficial bladder cancer.

When examining the asymptotic stable equilibrium of the system, i.e. how varying the doses of either BCG or IL-2 may affect immune cells, we found that BCG appears to directly influence activated the numbers of activated APCs –with which the bacteria directly interact– while effector lymphocyte numbers are almost independent of BCG. In contrast, the numbers of effector lymphocytes –which express IL-2 receptors– increase with increasing IL-2 dosages, whereas APCs, whether activated or not, remain level. These divergent effects of BCG and IL-2 may be the basis for the limited potentiating therapeutic effect, on BCG-infected tumor cells, of associating both.

We plan next to improve the model in which we will integrate other cells such as NK cells, as discussed above, and examine whether INF-α_{2B} or even IL-12, as recently proposed (Lee et al., 2004; Zaharoff et al., 2009) might potentiate BCG therapeutic efficacy (Arnold et al., 2004) in the absence or presence of IL-2.

Author's personal copy

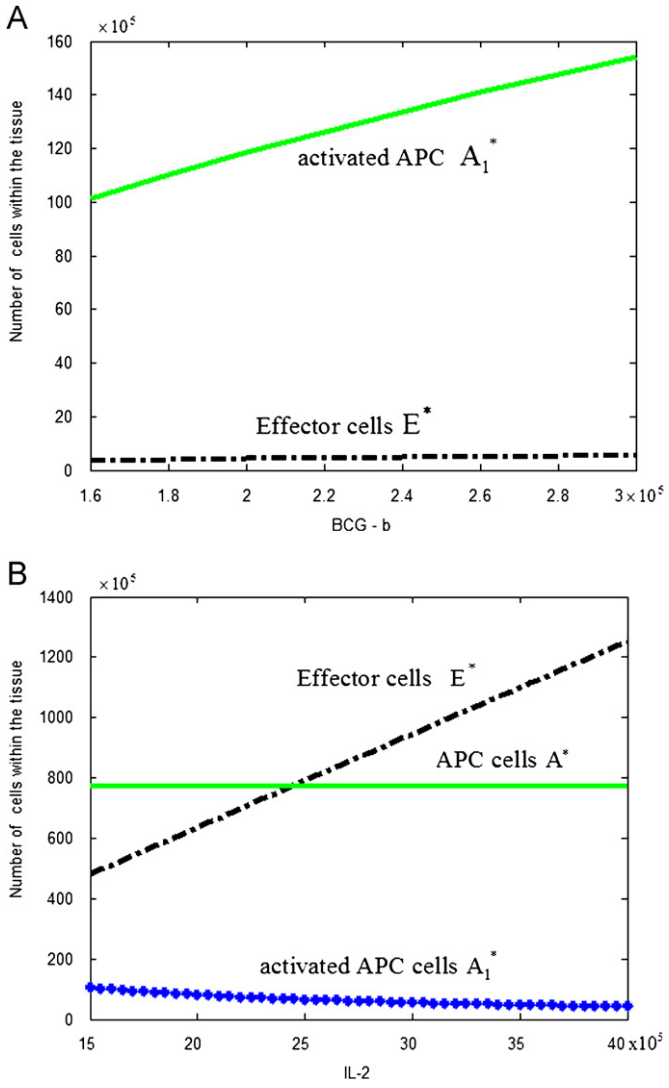

Fig. 11. Asymptotic stable equilibrium of immune cells in relation with the amounts of BCG or IL-2 administered. (A) Effect of varying BCG doses b on effector lymphocytes E^* and activated APCs A_1^* equilibrium levels. (B) Effect of varying IL-2 doses i_2 on effector lymphocytes E^* and APCs A, A_1^* equilibrium levels. Parameters are from Tables 2 and 3, with $r=0.028$.

Hopefully, these further extensions of the model could represent the basis for future mathematical studies of cancer dynamics that may guide clinical treatment. Indeed, using a similar experimental approach as Lee et al. (2004) with mice in which bladder cancer cells are implanted subcutaneously, it may be possible to validate and expand in vivo the results obtained with our 'in silico' model, though further investigations are required before the conclusions thus obtained are applicable to human bladder cancer.

Acknowledgments

Svetlana Bunimovich-Mendrazitsky thanks Professors Lewi Stone and Helen Byrne for fruitful and stimulating discussions. The primary model has been developed while visiting Nottingham University (UK) and working with Professor Helen Byrne. We are grateful to Professor Leonid Hanin for fruitful and stimulating discussions. Part of this study was supported by a fellowship from the Edmond J. Safra Bioinformatics program at Tel-Aviv University. We gratefully acknowledge the financial assistance received from the British Council through the Research Exchange Programme with Nottingham University.

Appendix A.

A.1. Local existence and uniqueness of problem (8) solution

Existence and uniqueness of problem (8) solution is standard if one restricts the result to a local one. Indeed, due to Cauchy-Lipschitz theorem (see for example, Schatzman, 2002), we have the following result:

Theorem 1.1. *Let T denotes any real positive number, A_0 and T_{u0} two initial conditions. Then, there exists one and only one solution $(B, A, A_1, E, I_2, T_i, T_u)$ to problem (8) which belongs to $[C^1([0,T])]^7$.*

Proof. Local existence and uniqueness of problem (8) solution on any finite interval $[0,T]$ is a consequence of the following property:

Let us represent the problem (8) in the formal presentation (A.1) given by:

$$\begin{cases} \text{Find } X \in R^d \text{ solution to :} \\ \frac{dX}{dt} = f(t,X), \\ X(0) = X_0, \end{cases} \tag{A.1}$$

where, in the case of problem (8), $d=7$ and X denotes the vector (B,A,A_1,E,I_2,T_i,T_u).which belongs to R^7.

So, because in the problem (8), the interaction between the components $(X_i)_{i=1,7}$ of the unknown X of (A.1) has mainly the structure X_iX_j, the function f is obviously C^1 which implies that it also locally satisfies Lipschitz condition.

Then, direct application of Cauchy–Lipschitz (Schatzman, 2002) leads to the result of existence and uniqueness of the solution to problem (8), on any finite interval $[0,T]$. □

A.2. Positive solutions

Positivity of problem (8) solution results from the following general theorem.

Theorem 2.1. *Let F be a real function defined on $[0,+\infty[$ which belongs to $C^1([0,+\infty[)$, solution to:*

$$\begin{cases} F'(t)+\alpha(t)F(t) = \beta(t), \quad t \in]0,+\infty[, \\ F(0) = F_0, \end{cases} \tag{A.2}$$

where α is a given function which belongs to $L^1([0,+\infty[)$, β is a positive function defined on $[0,+\infty[$, "sufficiently regular", and F_0 a given positive real number.

Then, F is positive on $[0,+\infty[$.

Proof. Let F be a solution to the problem (A.2). We multiply the differential equation by the integrating factor $\exp(\int_0^t \alpha(s)ds)$ and we get:

$$\frac{d}{dt}\left[F(t).\exp\left(\int_0^t \alpha(s)ds\right)\right] = \beta(t).\exp\left(\int_0^t \alpha(s)ds\right) \geq 0.$$

Then, $F(t).\exp(\int_0^t \alpha(s)ds)$is a monotonically increasing function and we have:

$$\forall t \in [0,+\infty[: F(t).\exp\left(\int_0^t \alpha(s)ds\right) \geq F(0) \geq 0.$$

Thus, F is positive on $[0,+\infty[$. □

Remark. To use Theorem 1.2, the main property we have to check is the positivity of the right hand β.

We are now in position to formulate the result dedicated to the positivity of problem (8) solution.

Author's personal copy

Theorem 2.2. *For any initial positive conditions A_0 and T_{u_o} associated to problem* (8)*, each component of the solution (B,A,A_1,E,I_2,-T_i,T_u) to problem* (8) *is positive.*

Proof. We begin with equation (7) of problem (8) which can directly be written:

$$T_u(t) = T_{u_0}\exp\left(\int_0^t (r - p_2 B)\,ds\right).$$

Taking into account that T_{u0} is positive, we get that $T_u(t) \geq 0, \forall t \in [0, +\infty[$.

- We consider now equation (1) of problem (8) and we set:
  $\alpha \equiv p_2 T_u + p_1 A + \mu_B$ and $\beta \equiv b\sum_{n=0}^{N-1}\delta(t - n\tau)$.
  So, because b is a given positive parameter, then β is positive and Theorem 2.1 gives that B is also positive.
- Concerning solution A to equation (2) of problem (8) we set:
  $\alpha \equiv (p_1 - \eta)B + \mu_A$ and $\beta \equiv \gamma \geq 0$.
  Then, Theorem 2.1 implies that $A$is positive.
- Equation (3) of problem (8) gives the same if one sets:
  $\alpha \equiv p_3 E + (\beta_1 + \mu_{A1})$ and $\beta \equiv p_1 AB$.
  Here, we get the positivity of β using the previous results concerning positivity of A and B.
  Therefore, Theorem 2.1 implies that A_1 is a positive function.
- We now jump to equation (5) of problem (8) and we set:
  $\alpha \equiv q_2 + \mu_{I2}$ and $\beta \equiv q_1 A_1 + i_2\sum_{n=0}^{N-1}\delta(t - n\tau)$.
  Because we assume that i_2 is positive and thanks to the previous result regarding the positivity of A_1, Theorem 2.1 implies that I_2 is positive too.
- We are now in position to treat solution E to Eq. (4) of problem (8). Here, we set:
  $\alpha \equiv \mu_E + p_5 T_i + p_4 A_1$ and $\beta \equiv \beta A_1 I_2$.
  As A_1 and I_2 are both positive, then we get from Theorem 2.1 that E is also positive.
- Let us finally consider solution T_i to equation (6) of problem (8) and let us set:
  $\alpha \equiv p_6 E$ and $\beta \equiv p_2 B T_u$.
  As B and T_u are both positive functions so, T_i is also positive due to Theorem 2.1. □

A.3. A priori estimation: Asymptotic behavior of problem (8) solution

This section is dedicated to the asymptotic behavior of problem (8) solution. We begin with a general theorem which assures that solution of linear differential equation is bounded on the interval $[0, +\infty[$.

Theorem 3.1. *Let α and β two given functions defined on $[0, +\infty[$. We assume the two following properties:*

- *α is a function which belongs to $L^1_{loc}([0, +\infty[)$ and it exists a real number α_0 such that $\forall t \in [0, +\infty[: \alpha(t) \geq \alpha_0 > 0$.*
- *The function β belongs to $L^\infty([0, +\infty[)$.*

Let F be a real function defined on $[0, +\infty[$ solution to the following problem:

$$\begin{cases} F'(t) + \alpha(t)F(t) = \beta(t), & t \in]0, +\infty[, \\ F(0) = F_0, \end{cases} \tag{A.3}$$

where F_0 is a given real number.
Then, F belongs to $L^\infty([0, +\infty[)$.

Proof. We multiply the differential equation of (A.3) by the integrating factor$\exp\left(\int_0^t \alpha(s)\,ds\right)$.

Then, we get after integration: $\forall t \in]0; +\infty[$:

$$F(t) = F(0)\exp\left(-\int_0^t \alpha(s)\,ds\right) + \int_0^t \beta(s)\exp\left(-\int_t^s \alpha(u)\,du\right)ds. \tag{A.4}$$

The control of the right hand of (A.4) is as follows:

- Because we assume that $\forall t \in [0, +\infty[: \alpha(t) \geq \alpha_0 > 0$ we get:
  $$F(0)\exp\left(-\int_0^t \alpha(s)ds\right) \leq F(0)e^{-\alpha_0 t}. \tag{A.5}$$
- On the other hand, the second term in (A.5) can be controlled by:
  $$\left|\int_0^t \beta(s)\exp\left(-\int_t^s \alpha(u)\,du\right)ds\right| \leq \|\beta\|_\infty \int_0^t \exp\left(-\alpha_0\int_t^s du\right)ds \leq \|\beta\|_\infty \frac{[1 - e^{\alpha_0 t}]}{\alpha_0}, \tag{A.6}$$
  where $\|\,.\,\|_\infty$ denotes the L^∞-norm defined by:
  $\|f\|_\infty \equiv \inf\{C \geq 0 \ \textit{such that}\ |f(x)| \leq C, \textit{a.e. on}\ [0, +\infty[\}$.

Then, from (A.5) and (A.6), we conclude that F belongs to$L^\infty([0, +\infty[)$.
We are now in position to give the main result of this section concerning the asymptotic behavior of problem (8) solution. □

Theorem 3.2. *Let (B,A,A_1,E,I_2,T_i,T_u) be the solution to problem* (8) *for a given pair of initial conditions A_0 and T_{u_0}. Then, (B,A,A_1,E,I_2) belongs to $[L^\infty([0, +\infty[)]^5$ and (T_i,T_u) belongs to $[L^\infty([0,T])]^2$, for any $T > 0$.*

Proof.

- First of all, we remark that due to Theorem 1.1, solution to problem (8) belong to $[C^1([0,T])]^7$.
  As a consequence, each of the seven unknowns of problem (8) belong to $L^\infty([0,T])$, for any $T > 0$. This is particularly the case for T_i and T_u.
  Let us now consider the unknowns (B,A,A_1,E,I_2) to problem (8). To prove that each of the five previous components belongs to$L^\infty([0, +\infty[)$, we will use Theorem 2.2 on the one hand, and Theorem 3.1, on the other hand.
- We begin by considering solution B to Eq. (1) of problem (8) and let us set the two functions α and β of Theorem 3.1 as follows:
  $\alpha \equiv p_2 T_u + p_1 A + \mu_B$ and $\beta \equiv b\sum_{n=0}^{N-1}\delta(t - n\tau)$.
  Then, because Theorem 2.2 which assures the positivity of T_u and A, we have:
  $p_2 T_u + p_1 A + \mu_B \geq \mu_B > 0$.
  Moreover, it is clear that β defined above belongs to $L^\infty([0, +\infty[)$. To use theorem 3.1 we only have to set that $\alpha_0 \equiv \mu_B$ and this allows us to conclude that B belongs to $L^\infty([0, +\infty[)$.
- The same idea is applied for solution A to equation (2) of problem (8) if one sets:
  $\alpha \equiv \mu_A + (p_1 - \eta)B$ and $\beta \equiv \gamma$.
  Here, one has to remark that regarding the parameters values of η and p_1 the difference $(p_1 - \eta)$ is strictly positive.
  Then, because B is also positive due to Theorem 2.2, and having

Author's personal copy

noticed that β is obviously bounded, we apply Theorem 3.1 and A belongs to $L^\infty([0,+\infty[)$.

- Regarding solution A_1 to equation (3) of problem (8), we set: $\alpha \equiv p_3E+(\beta_1+\mu_{A_1})$ and $\beta \equiv p_1AB$.

  Having shown that A and B belong to $L^\infty([0,+\infty[)$, then β also belongs to$L^\infty([0,+\infty[)$.
  Moreover, because E is positive due to Theorem 2.2, we simply control α as follows:
  $\alpha \equiv p_3E+(\beta_1+\mu_{A_1}) \geq \beta_1+\mu_{A_1} \equiv \alpha_0 > 0$.

  Consequently, Theorem 3.1 yields that A_1 belongs to $L^\infty([0,+\infty[)$.
- We jump one more time to equation (5) of problem (8) to control the solution I_2. Then, in this case, we consider the two functions α and β as follows:
  $\alpha \equiv q_2+\mu_{I_2}$ and $\beta \equiv q_1A_1+i_2\sum_{n=0}^{N-1}\delta(t-n\tau)$.

  Here, the application of Theorem 3.1 is immediate because we just got that A_1 belongs to $L^\infty([0,+\infty[)$. So, β is also a function of $L^\infty([0,+\infty[)$ and we also have:
  $\alpha \equiv q_2+\mu_{I_2} \geq \mu_{I_2} > 0$.

  This allows us to conclude that I_2 belongs to $L^\infty([0,+\infty[)$.
- To finish the proof of Theorem 3.2, we have to consider the unknown E, solution to equation (4) of problem (8) and we set: $\alpha \equiv \mu_E+p_5T_i+p_4A_1$ and $\beta \equiv \beta A_1I_2$.

  Inspection of α immediately shows that we get:
  $\alpha \equiv \mu_E+p_5\,T_i+p_4A_1 \geq \mu_E \equiv \alpha_0 > 0$,
  where we used that T_i and A_1 are both two positive functions due to Theorem 2.2.
  Moreover, it is clear that β is bounded on $[0,+\infty[$ as A_1 and I_2 belong to $L^\infty([0,+\infty[)$.
  So, from Theorem 3.1, E is also a function of $L^\infty([0,+\infty[)$. □

References

Aranha, O., Wood, D.P., Sarkar, F.H., 2000. Ciprofloxacin mediated cell growth inhibition, S/G2-M cell cycle arrest, and apoptosis in a human transitional cell carcinoma of the bladder cell line. Clin. Cancer Res. 6, 891–900.

Archuleta, J., Mullens, P., Primm, T.P., 2002. The relationship of temperature to desiccation and starvation tolerance of the Mycobacterium avium complex. Arch. Microbiol. 178, 311–314.

Arciero, J.C., Jackson, T.L., Kirschner, D.E., 2004. A mathematical model of tumor-immune evasion and siRNA treatment. Discret Contin Dyn. S B 4, 39–58.

Arnold, J., de Boer, E.C., O'Donnell, M.A., Bohle, A., Brandau, S., 2004. Immunotherapy of experimental bladder cancer with recombinant BCG expressing interferon-gamma. J Immunother. 2, 116.

Banerjee, S., 2008. Immunotherapy with interleukin-2: a study based on Mathematical modeling. Int. J. Appl. Math. Comput. Sci. 18 (No. 3), 389–398.

Berke, G., 1994. The binding and lysis of target cells by cytotoxic lymphocytes: molecular and cellular aspects. Annu. Rev. Immunol. 12, 735–773.

Bevers, R.F.M., Kurth, K.H., Schamhart, D.J.H., 2004. Role of urothelial cells in BCG immuno-therapy for superficial bladder cancer. Brit. J. cancer 91, 607–612.

Bohle, A., Brandau, S., 2003. Immune mechanisms in bacillus Calmette–Guerin immunotherapy for superficial bladder cancer. J Urol. 170, 964–969.

Bunimovich-Mendrazitsky, S., Shochat, E., Stone, L., 2007. Mathematical Model of BCG Immunotherapy in Superficial Bladder Cancer. Bull Math Biol. 69, 1847–1870.

Bunimovich-Mendrazitsky, S., Byrne, H., Stone, L., 2008. Mathematical Model of Pulsed Immunotherapy for Superficial Bladder Cancer. Bull Math Biol. 70 (7), 2055–2276.

Cappuccio, A., Elishmereni, M., Agur, Z., 2006. Immunotherapy by IL-21: potential treatment strategies evaluated in a mathematical model. Cancer Res. 66 (14), 7293–7300.

Castiglione, F., Piccoli, B., 2006. Optimal Control in a Model of Dendritic Cell Transfection Cancer Immunotherapy. Bulletin of Mathematical Biology 68, 255–274.

Castiglione, F., Piccoli, B., 2007. Cancer immunotherapy, mathematical modeling and optimal control. J. Theoret. Biol. 247, 723–732.

Cheng, C.W., Ng, M.T., Chan, S.Y., Sun, W.H., 2004. Low dose BCG as adjuvant therapy for superficial bladder cancer and literature review. Anz Journal of Surgery. 74 (7), 569–572.

Chopin, D., Gattegno, B., 2002. Superficial bladder tumors. Eur. Urol. 42, 533–541.

de Boer, E.C., de Jong, W.H., Steerenberg, P.A., et al., 1992. Induction of urinary interleukin-1 (IL-1), IL-2, IL-6, and tumor necrosis factor during intravesical immunotherapy with bacillus Calmette-Guérin in superficial bladder cancer. Cancer Immunol Immunother. 34 (306–312).

de Boer, R.J., Ganusov, V.V., Milutinovic, D., Hodgkin, P.D., Perelson, A.S., 2006. Estimating lymphocyte division and death rates from CFSE data. Bull. Math. Biol. 68, 1011–1031.

de Pillis, L.G., Radunskaya, A.E., Wiseman, C.L., 2005. A validated mathematical model of cell-mediated immune response to tumor growth. Cancer Res. 65, 7950–7958.

de Pillis, L.G., Gu, W., Radunskaya, A.E., 2006. Mixed immunotherapy and chemotherapy of tumor: modeling, application and biological interpretations. J. Theor. Biol. 238, 841–862.

Gaffen, S.L., Liu, K.D., 2004. Overview of interleukin-2 function, production and clinical applications. Cytokines. 28, 109–123.

Glickman, M.S., Jacobs, W.R., 2001. Microbial pathogenesis of *Mycobacterium tuberculosis*: dawn of a discipline. Cell. 104, 477–485.

Isaeva, O.G., Osipov, V.A., 2009. Mathematical modelling of anti-tumour immune response: immunocorrective effect of weak centimetre electromagnetic waves. Computational and Mathematical Methods in Medicine 10 (3), 185–201.

Iori, F., Di Seri, M., De Nunzio, C., 2002. Long-term maintenance bacille Calmette-Guerin therapy in high-grade superficial bladder cancer. Urology 59, 414–418.

Kaempfer, R., Gerez, L., Farbstein, H., Madar, L., Hirschman, O., Nussinovich, R., Shapiro, A., 1996. Prediction of response to treatment in superficial bladder carcinoma through pattern of interleukin-2 gene expression. J. Clin. Oncol. 14 (6), 1778–1786.

Keilholz, U., Scheibenbogen, C., Stoelben, E., Saeger, H.D., Hunstein, W., 1994. Immunotherapy of metastatic melanoma with interferon-alpha and interleukin-2: Pattern of progression in responders and patients with stable disease with or without resection of residual lesions. European Journal of Cancer 30 A (7), 955–958.

Kim, J.C., Steinberg, G.D., 2001. The limits of bacillus Calmette-Guerin for carcinoma in situ of the bladder. J Urol. 165, 745–756.

Kirschner, D., Panetta, J., 1998. Modelling immunotherapy of the tumor-immune interaction. Journal of Mathematical Biology 37 (3), 235–252.

Knowles, M.A., 2006. Mar. Molecular subtypes of bladder cancer: Jekyll and Hyde or chalk and cheese? Carcinogenesis 27 (3), 361–373.

Kolev, M., 2003. Mathematical modelling of the competition between tumors and immune system considering the role of the antibodies. Math. Comput. Model 37, 1143–1152.

Kronenberg, M., 2005. Toward an understanding of nkt cell biology: progress and paradoxes. Annu. Rev. Immunol. 23, 877–900.

Kuznetsov, V.A., Makalkin, I.A., Taylor, M.A., Perelson, A.S., 1994. Nonlinear dynamics of immunogenic tumours: parameter estimation and global bifurcation analysis. Bull. Math. Biol. 56, 295–321.

Lämmle, M., Beer, A., Settles, M., Hanning, C., Schwaibold, H., Drews, C., 2002. Reliability of MR imaging-based virtual cystoscopy in the diagnosis of cancer of the urinary bladder. Am J Roentgenol. 178, 1483–1488.

Lee, C.F., Chang, S.Y., Hsieh, D.S., Yu, D.S., 2004. Immunotherapy for bladder cancer using recombinant bacillus Calmette-Guerin DNA vaccines and interleukin-12 DNA vaccine. J. Urol. 171, 1343–1347.

Ludewig, B., Krebs, P., Junt, T., Metters, H., Ford, N.J., Anderson, R.M., Bocharov, G., 2004. Determining control parameters for dendritic cell-cytotoxic T lymphocyte interaction. European. J. Immunol. 34, 2407–2418.

Malek, T.R., Bayer, A.L., 2004. Tolerance, not immunity, crucially depends on IL-2. Nat. Rev. Immunol. 4, 665–674.

Marino, S., Kirschner, D.E., 2004. The human immune response to Mycobacterium tuberculosis in lung and lymph node. J. Theor. Biol. 227, 463–486.

Martinez-Pineiro, J.A., Muntanola, P., 1977. Nonspecific immunotherapy with BCG vaccine in bladder tumors: a preliminary report. Eur. Urol. 3, 11–22.

Matzavinos, A., Chaplain, M.A., Kuznetsov, V.A., 2004. Mathematical modelling of the spatio-temporal response of cytotoxic T-lymphocytes to a solid tumour. Math Med. Biol. 21, 1–34.

Megiovanni, A.M., Sanchez, F., Robledo-Sarmiento, M., Morel, C., Gluckman, J.C., Boudaly, S., 2006. Polymorphonuclear neutrophils deliver activation signals and antigenic molecules to dendritic cells: a new link between leukocytes upstream of T lymphocytes. J. Leukoc. Biol. 79, 977–988.

Morales, A., Eidinger, D., Bruce, A.W., 1976. Intracavity Bacillus Calmette-Guérin in the treatment of superficial bladder tumors. J. Urol. 116, 180–183.

Morel, C., Badell, E., Abadie, V., Robledo, M., Setterblad, N., Gluckman, J.C., Gicquel, B., Boudaly, S., Winter, N., 2008. Mycobacterium bovis BCG–infected neutrophils and dendritic cells cooperate to induce specific T-cell responses in humans and mice. Eur. J. Immunol. 38, 437–447.

Nani, F., Freedman, H.I., 2000. A mathematical model of cancer treatment by immunotherapy. Math. Biosci. 163, 159–199.

Rosenberg, S.A., Lotze, M.T., 1986. Cancer immunotherapy using interleukin-2 and interleukin-2-activated lymphocytes. Annual Review of Immunology 4 (1), 681–709.

Rosenberg, S.A., 2008. Overcoming obstacles to the effective immunotherapy of human cancer. Proc. Natl. Acad. Sci. USA 105, 12643–12644.

Sakaguchi, S., Yamaguchi, T., Nomura, T., Ono, M., 2008. Regulatory T cells and immune tolerance. Cell. 133, 775–785.

Author's personal copy

Schatzman, M., 2002. Numerical analysis: a mathematical introduction. Oxford Univ. Press, p. 363.
Schwartzentruber, D.J., 1993. In vitro predictors of clinical response in patients receiving interleukin-2-based immunotherapy. Current Opinion in Oncology 5 (6), 1055–1058.
Shapiro, A., Gofrit, O., Pode, D., 2007. The treatment of superficial bladder tumor with IL-2 and BCG. J. Urol. (Supplement) 177 (4), 81.
Shochat, E., Hart, D., Agur, Z., 1999. Using computer simulations for evaluating the efficacy of breast cancer chemotherapy protocols. Mathematical Models and Methods in Applied Sciences 9 (4), 599–615.
Schwartz, L., 1966. Mathematics for the Physical Sciences, Hermann, Paris. Addison-Wesley, Reading, MA Rev. Ed.
Suttmann, H., Jacobsen, M., Reiss, K., Jocham, D., Bohle, A., Brandau, S., 2004. Mechanisms of bacillus Calmette-Guerin mediated natural killer cell activation. J. Urol. 172, 1490.
Spratt, J.A., Von Fournier, D., Spratt, J.S., Weber, E.E., 1993. Decelerating growth and human breast cancer. Cancer 71, 2013–2019.
Tailleux, L., Neyrolles, O., Honoré-Bouakline, S., Perret, E., Sanchez, F., Abastado, J.P., Lagrange, P.H., Gluckman, J.C., Rosenzwajg, M., Herrmann, J.L., 2003. Constrained intracellular survival of Mycobacterium tuberculosis in human dendritic cells. J. Immunol. 170, 1939–1948.
Wigginton, J., Kirschner, D., 2001. A model to predict cell-mediated immune regulatory mechanisms during human infection with Mycobacterium tuberculosis. J. Immunol. 166, 1951–1967.
Yutkin, V., Pode, D., Pikarsky, E., Mandelboim, O., 2007. The expression level of ligands for natural killer cell receptors predicts response to bacillus Calmette-Guerin therapy: a pilot study. J Urol. 178, 2660–2664.
Zagury, D., Bernard, J., Dufer, J., 1975. Biology of isolated immunocytes. Isolation into a closed liquid microchamber - application to PFS. ANNALES D IMMUNOLOGIE. C126 (1), 23–30.
Zaharoff, D.A., Hoffman, B.S., Hooper, H.B., Benjamin Jr., C.J., Khurana, K.K., Hance, K.W., Rogers, C.J., Pinto, P.A., Schlom, J., Greiner, J.W., 2009. Intravesical immunotherapy of superficial bladder cancer with chitosan/interleukin-12. Cancer Res. 69, 6192–6199.
Wodarz, D., Jansen, V.A.A., 2003. A dynamical perspective of ctl cross-priming and regulation: implications for cancer immunology. Immunol. Lett. 86, 213–227.